NATIONAL INSTITUTE OF POLAR RESEARCH

ANTARCTIC GEOLOGICAL MAP SERIES
SHEET 31 BALCHENFJELLA

Explanatory Text of Geological Map of Balchenfjella, Sør Rondane Mountains, Antarctica

Masao ASAMI, Hiroshi MAKIMOTO, E.S. GREW,
Yasuhito OSANAI, Yuhei TAKAHASHI, Noriyoshi TSUCHIYA,
Yoshiaki TAINOSHO and Kazuyuki SHIRAISHI

NATIONAL INSTITUTE OF POLAR RESEARCH
TOKYO, MARCH 1991

National Institute of Polar Research
9-10, Kaga 1-chome, Itabashi-ku
Tokyo 173, Japan

Errata:

Please replace Table 1 on page 4 of the Explanatory Text with this corrected Table.

Table 1. Mineral assemblages of metamorphic rocks in the Balchenfjella area.

A. Biotite-hornblende gneiss
A1. Hbl+Bt+Pl+Qtz±Kfs
A2. Cpx+Hbl+Bt+Pl+Qtz [±Cum]
A3. Cpx+Hbl+Bt+Pl+Kfs+Qtz
A4. Grt+Hbl+Bt+Pl+Qtz [±Cum]
A5. Grt+Hbl+Bt+Pl+Kfs+Qtz
A6. Grt+Cpx+Hbl+Bt+Pl+Qtz [±Cum]
A7. Grt+Cpx+Hbl+Bt+Pl+Kfs+Qtz
A8. Grt+Opx+Hbl+Bt+Pl+Qtz
<Ap, Zrn, Opq; ±Aln, Spn>

B. Hornblende gneiss
B1. Hbl+Bt+Pl+Qtz [±Cum]
B2. Cpx+Hbl+Bt+Pl+Qtz±Kfs
B3. Opx+Hbl+Bt+Pl [Cum]
B4. Opx+Hbl+Bt+Pl+Qtz
B5. Opx+Cpx+Hbl+Bt+Pl±Qtz [Cum]
B6. Grt+Hbl+Bt+Pl+Qtz [Cum]
B7. Grt+Hbl+Bt+Pl+Kfs+Qtz
B8. Grt+Cpx+Hbl+Bt+Pl+Qtz
<Ap, Zrn, Opq; ±Aln, Spn>

C. Garnet-biotite gneiss and biotite gneiss
C1. Grt+Bt+Pl+Qtz (±Sp)
C2. Grt+Bt+Pl+Kfs+Qtz (±Sp, Sil)
C3. Sil+Grt+Bt+Pl+Qtz (Sp) [±Hög]
C4. Sil+Grt+Bt+Pl+Kfs+Qtz (Sp)
C5. Ghn+Grt+Bt+Pl+Qtz+Sp±Kfs
C6. Grt+Opx+Bt+Pl+Qtz [Cum]
C7. Bt+Pl+Kfs+Qtz
C8. Sp+Grt+Bt+Pl (Sil) [Hög, Mrg, Chl]
C9. Crn+Sp+Grt+Bt+Pl (Ky, Ged, Qtz)
C10. Crn+Sp+Grt+Bt+Pl (Sil) [Mrg]
C11. Crn+Sp+Sil+Grt+Bt+Pl (St)
C12. Crn+Sp+Sil+Grt+Bt+Pl+Kfs
C13. Crn+Bt+Pl±Kfs [Mrg]
<Ap, Zrn, Opq; ±Rt, Mnz, Aln>

D. Charnockitic gneiss
D1. Opx+Bt+Pl+Kfs+Qtz
D2. Opx+Hbl+Bt+Pl+Kfs+Qtz
D3. Opx+Cpx+Hbl+Bt+Pl+Kfs+Qtz
D4. Cpx+Hbl+Bt+Pl+Kfs+Qtz
D5. Opx+Bt+Pl+Qtz [Cum]
<Ap, Zrn, Opq>

E. Marble and calc-silicate rocks
a. Marble
E1. Sp+Fo+Phl+Cal+Dol [±Chu, Chl, Aln]
E2. Sp+Fo+Phl+Cal+Dol [Chu, Tr; ±Chl]
E3. Sp+Fo+Cpx+Tr+Phl+Cal+Dol
E4. Cpx+Pg+Phl+Cal
<Ap, Opq; ±Rt>
b. Calc-silicate rocks
E5. Grt+Cpx+Hbl+Scp+Cal+Qtz+Spn [Ep]
E6. Grt+Cpx+Scp+Cal+Qtz+Spn+Aln [Ep]
E7. Cpx+Hbl+Scp+Cal+Kfs+Qtz+Spn [Ep]
E8. Cpx+Tr+Pl+Scp+Cal+Fl [Ep, Prh, Ms]
E9. Scp+Cal+Pl+Kfs+Qtz+Spn [Ep]
<±Zrn, Ap, Opq>

F. Ultramafic rocks
F1. Opx+Cum+Bt
F2. Opx+Cum+Hbl+Bt
F3. Opx+Cpx+Hbl+Bt
F4. Fo+Opx+Bt
F5. Fo+Opx+Cum+Ath+Hbl+Bt
F6. Ol+Opx+Hbl+Sp+Bt±Cpx
F7. Cpx+Hbl+Bt
<Ap, Opq; ±Zrn, Aln>

G. Amphibolite
G1. Hbl+Bt+Pl±Qtz
G2. Cpx+Hbl+Bt+Pl
G3. Cpx+Hbl+Pl
G4. Opx+Hbl+Bt+Pl [±Cum]
G5. Opx+Cpx+Hbl+Bt+Pl [±Cum]
G6. Grt+Hbl+Bt+Pl [±Cum]
G7. Grt+Cpx+Hbl+Pl+Qtz
G8. Grt+Cpx+Hbl+Bt+Pl [±Cum]
G9. Grt+Cpx+Hbl+Bt+Pl+Kfs
G10. Grt+Cpx+Hbl+Bt+Pl±Cum
G11. Grt+Cpx+Hbl+Bt+Pl+Qtz±Cum
G12. Grt+Cpx+Hbl+Bt+Pl+Kfs+Qtz
G13. Grt+Opx+Hbl+Bt+Pl [±Cum]
G14. Grt+Opx+Hbl+Bt+Pl+Qtz

Explanatory Text of Geological Map of Balchenfjella, Sør Rondane Mountains, Antarctica

Masao ASAMI[1], Hiroshi MAKIMOTO[2], Edward S. GREW[3], Yasuhito OSANAI[4], Yuhei TAKAHASHI[2], Noriyoshi TSUCHIYA[5], Yoshiaki TAINOSHO[6] and Kazuyuki SHIRAISHI[7]

1. Balchenfjella

The Sør Rondane Mountains (71°40'-72°30'S; 21°45'-28°E) are an about 250 km-long, 100 km-wide, wedge-shaped range in East Queen Maud Land, and include peaks of more than 3000 m above sea level. All outcrops studied consist of crystalline rocks of the East Antarctic shield. In the mountains, the eastern Sør Rondane Mountains, which lie east of Byrdbreen (around 26°30'E), include a large exposure, Balchenfjella (Balchen Mountain), and numerous nunataks. This sheet covers a substantial area of the eastern Sør Rondane Mountains: Balchenfjella consisting of Gropeheia and Berrheia, and surrounding nunataks including Austrabbane, Isklakken, Trillingane, Hesteskoen, Firlingane, Bulken and Isrosene.

The Sør Rondane Mountains were discovered from the air in 1937 during the Norwegian expedition of Lars Christensen. The mountains were first surveyed in 1958 and then in 1959, 1960 and 1965 by Belgian geologists. Their reconnaissance surveys were made over a wide area of the mountains, including the northern nunataks in the eastern Sør Rondane Mountains, and they reported their geological and geochronological results (VAN AUTENBOER *et al.*, 1964; PICCIOTTO *et al.*, 1964; VAN AUTENBOER, 1969; PASTEELS and MICHOT, 1970; VAN AUTENBOER and LOY, 1972). Soviet geologists of the 1966-1967 expedition also briefly surveyed part of the Sør Rondane Mountains (RAVICH and KAMENEV, 1972).

---

1) Department of Geological Sciences, College of Liberal Arts, Okayama University, 1-1, Tsushima Naka 2-chome, Okayama 700.
2) Geological Survey of Japan, 1-3, Higashi 1-chome, Tsukuba 305.
3) Department of Geological Sciences, University of Maine, 110 Boardman Hall, Orono, Maine 04469, U. S. A.
4) Department of Earth Sciences and Astronomy, Fukuoka University of Education, 729, Akama, Munakata, Fukuoka 811-41.
5) Department of Resources Engineering, Faculty of Engineering, Tohoku University, Aramaki, Aoba-ku, Sendai 980.
6) Department of Geology, Faculty of Education, Kobe University, 1-33 Tsuruko, Nada-ku, Kobe 657.
7) National Institute of Polar Research, 9-10, Kaga 1-chome, Itabashi-ku, Tokyo 173.

Since the twenty-fifth Japanese Antarctic Research Expedition (JARE-25) in 1984, geological field work in the Sør Rondane Mountains had been carried out by Japanese geologists every summer through JARE-28 (1987). They had extensively surveyed the western and central Sør Rondane Mountains, and had characterized the geological, petrographic and geochronological features of the metamorphic and plutonic rocks (KOJIMA and SHIRAISHI, 1986; ASAMI and SHIRAISHI, 1987; ISHIZUKA and KOJIMA, 1987; SHIRAISHI and KOJIMA, 1987; TAKIGAMI *et al.*, 1987; OSANAI *et al.*, 1988, 1990; SAKIYAMA *et al.*, 1988; SHIRAISHI *et al.*, 1988, 1991; SHIRAISHI and KAGAMI, 1989; TAKAHASHI *et al.*, 1990). However, a substantial portion of the eastern Sør Rondane Mountains had not been geologically surveyed prior to 1987.

We, members of JARE-29 (M.A., H.M. and E.S.G.) and JARE-31 (Y.O., Y.T., N.T., Y.T. and K.S.), performed geological surveys in the eastern Sør Rondane Mountains during the summer of 1988 and 1990, respectively. In addition, K.S. conducted a supplementary geological survey in November, 1990. Some geological, petrological and mineralogical results have been published (ASAMI *et al.*, 1988, 1989, 1990; GREW *et al.*, 1988, 1989a, b; MAKIMOTO *et al.*, 1990).

Geomorphologically Balchenfjella is very unique in the Sør Rondane Mountains. Balchenfjella is characterized by landforms of areal scouring owing to continental ice-sheet glaciation and most of the area still lies below the surrounding ice surface, while the other massifs and nunataks show alpine features and are standing out above the general surrounding ice surfaces (ANIYA, 1989; HAYASHI and MIURA, 1989).

2. Outline of Geology

The exposures examined in the Balchenfjella area are composed of high-grade gneissic rocks accompanied by migmatite and small bodies of intrusive rocks. The intrusive rocks are mostly granite and pegmatite occurring as dikes and veins; a diorite intrusive constitutes a small nunatak. Granite also occurs as neosomes in migmatite. The absence of large intrusive masses is characteristic of the eastern Sør Rondane and contrasts with the western and central Sør Rondane Mountains where large masses of acid to intermediate plutonic rocks have been mapped (VAN AUTENBOER, 1969; KOJIMA and SHIRAISHI, 1986; ISHIZUKA and KOJIMA, 1987; SHIRAISHI and KOJIMA, 1987; SAKIYAMA *et al.*, 1988). Geological structure of the metamorphic rocks is complex due to the combined effects of folding and migmatization.

Rb-Sr biotite ages of 447 Ma and 450 Ma were obtained on amphibole-biotite gneiss and leucocratic pegmatite, respectively, from Trillingane nunataks, suggesting a late Ordovician age for plutonic activity (VAN AUTENBOER, 1969). 400-550 Ma ages are known over a wide area of the Sør Rondane Mountains (VAN AUTENBOER, 1969; KOJIMA and SHIRAISHI, 1986; TAKIGAMI *et al.*, 1987; TAKAHASHI *et al.*, 1990). Recently in the central and western Sør Rondane Mountains, late Proterozoic, high-grade metamorphic and plutonic events have been suggested by whole rock ages of 999 Ma (Sm-Nd) and 1167 Ma (Rb-Sr) on granulite-facies gneiss (SHIRAISHI and KAGAMI, 1989) and a whole rock age of 956 Ma (Rb-Sr) on tonalite (TAKAHASHI *et al.*, 1990).

The rocks of the Balchenfjella area can be classified into the following types on the basis of the mode of occurrence, lithology and mineral assemblages.

A. Metamorphic rocks
  A-1. Rocks of presumed sedimentary and volcanogenic origin
    (1) Biotite-hornblende gneiss
    (2) Hornblende gneiss
    (3) Garnet-biotite gneiss and biotite gneiss
    (4) Charnockitic gneiss
    (5) Marble and calc-silicate rocks
  A-2. Rocks of presumed magmatic origin
    (1) Ultramafic rocks
    (2) Amphibolite and pyroxene granulite (= metabasite)
    (3) Metagabbro
    (4) Cummingtonite gneiss
    (5) Metadike rocks
  A-3. Migmatite
B. Unmetamorphosed plutonic rocks
    (1) Diorite
    (2) Granite and pegmatite

3. Metamorphic Rocks

The metamorphic rocks consist largely of biotite-hornblende gneiss and subordinate amphibolite, hornblende gneiss, garnet-biotite gneiss and biotite gneiss. These rocks are commonly migmatized by development of granitic neosomes, and intensively migmatized rocks are mapped as migmatite. Charnockitic gneiss is restricted to the southern part of the area. Marble, calc-silicate rocks, ultramafic rocks, pyroxene granulite, metagabbro and cummingtonite gneiss are local. Metadike rocks are recognized in seven localities.

Geological and petrographic characteristics suggest that five types of metamorphic rocks are derived from sedimentary and volcanogenic precursors, while the remaining rocks have an igneous parentage. Mineral assemblages of rocks of A-1 and A-2 are given in Table 1.

Table 1. Mineral assemblages of metamorphic rocks in the Balchenfjella area.

A. Biotite-hornblende gneiss
A1. Hb+Bi+Pl+Qu±Kf
A2. Cp+Hb+Bi+Pl+Qu [±Cum]
A3. Cp+Hb+Bi+Pl+Kf+Qu
A4. Ga+Hb+Bi+Pl+Qu [±Cum]
A5. Ga+Hb+Bi+Pl+Kf+Qu
A6. Ga+Cp+Hb+Bi+Pl+Qu [±Cum]
A7. Ga+Cp+Hb+Bi+Pl+Kf+Qu
A8. Ga+Op+Hb+Bi+Pl+Qu
<Ap, Zr, Opq; ±Aln, Sph>

B. Hornblende gneiss
B1. Hb+Bi+Pl+Qu [±Cum]
B2. Cp+Hb+Bi+Pl+Qu±Kf
B3. Op+Hb+Bi+Pl [Cum]
B4. Op+Hb+Bi+Pl+Qu
B5. Op+Cp+Hb+Bi+Pl±Qu [Cum]
B6. Ga+Hb+Bi+Pl+Qu [Cum]
B7. Ga+Hb+Bi+Pl+Kf+Qu
B8. Ga+Cp+Hb+Bi+Pl+Qu
<Ap, Zr, Opq; ±Aln, Sph>

C. Garnet-biotite gneiss and biotite gneiss
C1. Ga+Bi+Pl+Qu (±Sp)
C2. Ga+Bi+Pl+Kf+Qu (±Sp, Sil)
C3. Sil+Ga+Bi+Pl+Qu (Sp) [±Hög]
C4. Sil+Ga+Bi+Pl+Kf+Qu (Sp)
C5. Ghn+Ga+Bi+Pl+Qu+Sphl±Kf
C6. Ga+Op+Bi+Pl+Qu [Cum]
C7. Bi+Pl+Kf+Qu
C8. Sp+Ga+Bi+Pl (Sil) [Hög, Mrg, Chl]
C9. Crn+Sp+Ga+Bi+Pl (Ky, Gd, Qu)
C10. Crn+Sp+Ga+Bi+Pl (Sil) [Mrg]
C11. Crn+Sp+Sil+Ga+Bi+Pl (St)
C12. Crn+Sp+Sil+Ga+Bi+Pl+Kf
C13. Crn+Bi+Pl±Kf [Mrg]
<Ap, Zr, Opq; ±Ru, Mnz, Aln>

D. Charnockitic gneiss
D1. Op+Bi+Pl+Kf+Qu
D2. Op+Hb+Bi+Pl+Kf+Qu
D3. Op+Cp+Hb+Bi+Pl+Kf+Qu
D4. Cp+Hb+Bi+Pl+Kf+Qu
D5. Op+Bi+Pl+Qu [Cum]
<Ap, Zr, Opq>

E. Marble and calc-silicate rocks
a. Marble
E1. Sp+Fo+Phl+Cc+Do [±Chu, Chl, Aln]
E2. Sp+Fo+Phl+Cc+Do [Chu, Tr; ±Chl]
E3. Sp+Fo+Cp+Tr+Phl+Cc+Do
E4. Cp+Prg+Phl+Cc
<Ap, Opq; ±Ru>
b. Calc-silicate rocks
E5. Ga+Cp+Hb+Sc+Cc+Qu+Sph [Ep]
E6. Ga+Cp+Sc+Cc+Qu+Sph+Aln [Ep]
E7. Cp+Hb+Sc+Cc+Kf+Qu+Sph [Ep]
E8. Cp+Tr+Pl+Sc+Cc+Fl [Ep, Prh, Mu]
E9. Sc+Cc+Pl+Kf+Qu+Sph [Ep]
<±Zr, Ap, Opq>

F. Ultramafic rocks
F1. Op+Cum+Bi
F2. Op+Cum+Hb+Bi
F3. Op+Cp+Hb+Bi
F4. Fo+Op+Bi
F5. Fo+Op+Cum+Anth+Hb+Bi
F6. Ol+Op+Hb+Sp+Bi±Cp
F7. Cp+Hb+Bi
<Ap, Opq; ±Zr, Aln>

G. Amphibolite
G1. Hb+Bi+Pl±Qu
G2. Cp+Hb+Bi+Pl
G3. Cp+Hb+Pl
G4. Op+Hb+Bi+Pl [±Cum]
G5. Op+Cp+Hb+Bi+Pl [±Cum]
G6. Ga+Hb+Bi+Pl [±Cum]
G7. Ga+Cp+Hb+Pl+Qu
G8. Ga+Cp+Hb+Bi+Pl [±Cum]
G9. Ga+Cp+Hb+Bi+Pl+Kf
G10. Ga+Cp+Hb+Bi+Pl±Cum
G11. Ga+Cp+Hb+Bi+Pl+Qu±Cum
G12. Ga+Cp+Hb+Bi+Pl+Kf+Qu
G13. Ga+Op+Hb+Bi+Pl [±Cum]
G14. Ga+Op+Hb+Bi+Pl+Qu

Table 1. (Continued)

G15. Grt+Opx+Cpx+Hbl+Bt+Pl [Cum]
G16. Grt+Opx+Cpx+Hbl+Bt+Pl+Qtz
<Ap, Zrn, Opa; ±Aln, Spn, Mnz, Rt>

H. Pyroxene granulite
H1. Grt+Cpx+Hbl+Bt+Pl+Qtz
H2. Grt+Opx+Cpx+Hbl+Bt+Pl+Qtz [Cum]
<Ap, Zrn, Opq>

I. Metagabbro
I1. Grt+Opx+Cpx+Hbl+Bt+Pl [Cum]
I2. Grt+Opx+Cpx+Hbl+Bt+Pl+Qtz [±Cum]
I3. Grt+Opx+Cpx+Hbl+Bt+Pl+Kfs+Qtz
I4. Opx+Cpx+Hbl+Bt+Pl+Qtz
I5. Grt+Hbl+Bt+Pl+Qtz [Cum]
<Ap, Zrn, Opq>

J. Cummingtonite gneiss
J1. Hbl+Bt+Pl [Cum]
<Ap, Zrn, Opq>

K. Metadike rocks
a. Amphibolite
K1. Grt+Hbl+Bt+Pl
K2. Grt+Hbl+Bt+Pl+Kfs+Qtz
K3. Grt+Cpx+Hbl+Bt+Pl+Qtz
K4. Grt+Opx+Cpx+Hbl+Bt+Pl±Qtz
<Ap, Zrn, Opq; ±Aln>

b. Biotitic schist
K5. Hbl+Bt+Pl+Qtz±Kfs
K6. Cpx+Hbl+Bt+Pl+Kfs+Qtz
<Ap, Spn, Opq>

Mineral abbreviations (mostly after KRETZ, 1983): Aln-allanite, Amp-amphibole, Ap-apatite, Ath-anthophyllite, Bt-biotite, Cal-calcite, Chl-chlorite, Chu-clinohumite, Cpx-clinopyroxene, Crn-corundum, Cum-cummingtonite, Dol-dolomite, Ep-epidote, Fl-fluorite, Fo-forsterite, Ged-gedrite, Ghn-gahnite, Grt-garnet, Hbl-hornblende, Hög-högbomite, Kfs-K-feldspar, Ky-kyanite, Mnz-monazite, Mrg-margarite, Ms-muscovite, Ol-olivine, Opx-orthopyroxene, Opq-opaque minerals, Pg-pargasite, Phl-phlogopite, Pl-plagioclase, Prh-prehnite, Qtz-quartz, Rt-rutile, Scp-scapolite, Sil-sillimanite, Sp-sphalerite, Spl-spinel, Spn-sphene, St-staurolite, Tr-tremolite, Zrn-zircon.
< >: Accessory minerals. ( ): Inclusions in minerals. [ ]: Later minerals.

3.1. Biotite-hornblende gneiss

The biotite-hornblende gneiss is the most abundant rock type. It is well-layered due to the alternation of biotite-hornblende-rich and quartzofeldspathic bands several millimeters to several centimeters thick (Plate 1A). Relative proportions of mafic and felsic minerals vary even within a band. This gneiss commonly alternates with amphibolite and hornblende gneiss and in places is accompanied by layers and lenses of garnet-biotite gneiss, calc-silicate rocks, marble and pyroxene granulite. Locally garnet is observable in the biotite-hornblende gneiss with the naked eye.

3.2. Hornblende gneiss

The occurrence of the hornblende gneiss is as widespread as the amphibolite. This gneiss forms concordant hornblende-rich layers, several centimeters to several tens of centimeters thick, in the biotite-hornblende gneiss (Plate 1B). Unlike the amphibolite, the gneiss is well-layered with felsic bands. This gneiss is also associated with some calc-silicate rocks. Garnet and clinopyroxene is often visible in outcrops of the gneiss.

3.3. Garnet-biotite gneiss and biotite gneiss

These gneisses include pelitic, quartzofeldspathic and feldspathic rocks enriched in biotite, garnet, sillimanite and rarely corundum, hercynite, or gahnite. They occur in 0.5 to 3 m-thick layers intercalated in the biotite-hornblende gneiss (Plate 1C). Seven localities of sillimanite-garnet-biotite gneiss have been found. The sillimanite gneiss layers are best developed at the northeast end of Berrheia, where staurolite has been found in a sillimanite-spinel-corundum-garnet-biotite gneiss (ASAMI *et al.*, 1990). Kyanite has been found in a garnet-plagioclase-biotite schist from the eastern part of Gropeheia (GREW *et al.*, 1990).

3.4. Charnockitic gneiss

The term charnockitic gneiss refers to quartzofeldspathic rocks containing orthopyroxene, which is to a variable extent replaced by cummingtonite. A dark-gray color on the broken rock surface is characteristic. This rock is commonly well-layered due to the alternation of felsic bands and more mafic bands (Plate 2A), but in places is poorly foliated. This gneiss occurs largely in the southern part of Berrheia. We did not succeed in locating a distinct contact between the biotite-hornblende gneiss and charnockitic gneiss; we infer this contact to be diffuse with mixing of the two rock types. Small lenses of two-pyroxene amphibolite are common in the charnockitic gneiss. Garnet is rarer in these lenses than in amphibolite from the northern part of the Balchenfjella area.

3.5. Marble and calc-silicate rocks

Marbles, which include calcitic and dolomitic varieties, occur mostly as concordant or subconcordant layers and lenses up to several tens of meters across in the biotite-hornblende gneiss (Plate 2B).

The calc-silicate rocks form small pods enclosed in the marble (Plate 2B), bands between the marble and adjacent gneisses, and layers and lenses up to a few meters across intercalated in the biotite-hornblende gneiss and amphibolite.

3.6. Ultramafic rocks

Ultramafics occur in lenses up to several meters across at four localities, and in a lenticular block about 100 m long near the north end of Berrheia.

At the three localities, these lenses occur in the biotite-hornblende gneiss (Plate 2C) and include olivine-rich rocks. At the other one, they occur in the migmatite in Berrheia (Plate 5A) and include rocks rich in cummingtonite and calcic clinoamphibole. Between these lenses and the host rocks, reaction zones of micas and amphiboles are developed.

The lenticular block is made up of clinopyroxenite and surrounded by quartzofeldspathic biotite-hornblende and garnet-biotite gneisses.

3.7. Amphibolite and pyroxene granulite

The amphibolite commonly occurs as dark-colored layers and lenses up to a few tens of meters across which are concordant or subconcordant with layers of the biotite-hornblende gneiss (Plate 3A), hornblende gneiss, garnet-biotite gneiss, biotite gneiss and charnockitic gneiss. Some amphibolite lenses are associated with the calc-silicate rocks. The amphibolite is not as well-banded as the other gneisses and in places is massive. Garnet, clinopyroxene and orthopyroxene commonly appear in the amphibolite.

The pyroxene granulite is typically developed in a northwest-trending, marble-bearing belt, which is about 1 km wide and extends at least 4 km along strike from the north end of Berrheia into Gropeheia. This rock is characteristically poorly foliated and dark-colored due to a dark gray color of plagioclase in addition to abundant mafic minerals such as garnet, clinopyroxene and orthopyroxene.

Pyroxene-bearing varieties of the amphibolite, together with pyroxene granulite and metagabbro, are grouped into mafic granulite in the separate petrology paper (GREW *et al.*, 1989).

3.8. Metagabbro

Metagabbro forms a lenticular body of resistant orthogneiss nearly a kilometer long within the migmatite belt near the north end of Berrheia (Plate 3B). It appears black from a distance, while close up, it is poorly foliated and dark-colored like the pyroxene granulite and charnockitic gneiss. Lath-shaped plagioclase crystals are occasionally observed on the weathered surface (Plate 3C).

3.9. Cummingtonite gneiss

This gneiss is characterized by cummingtonite knots developed in the plagioclase-rich matrix. The rock crops out at the northwest corner of Gropeheia and occurs as a concordant layer several meters thick in the biotite-hornblende gneiss. In places, garnet is sporadically observed in this rock.

The cummingtonite gneiss is also found in a nunatak (Austhamaren) north of this area, and contains a distinctive orthopyroxene having textures suggestive of inverted pigeonite. This gneiss, together with the older metadike rock mentioned below, is interpreted to be part of a pre-metamorphic plutonic complex intrusive into marble-bearing metasediments (GREW *et al.*, 1989).

3.10. Metadike rocks

The metadike rocks are clearly discordant with the country metamorphic rocks. Two types of the metadike rocks are distinguished; garnetiferous amphibolite and biotitic schist. These two were emplaced during different stages.

The older metadikes are biotitic garnetiferous amphibolite found at Hesteskoen. The rock is locally broken into lenses and is recrystallized as completely as the surrounding gneisses (Plate 4A). Metamorphic minerals include orthopyroxene and clinopyroxene, indicating that the dikes have been deformed and metamorphosed under the granulite-facies conditions.

The younger metadikes are biotitic schist found at six localities. The dikes crosscut typical gneissic rocks such as the biotite-hornblende gneiss and amphibolite. In general, the crosscutting relationship of the dikes has not been destroyed by later deformation (Plate 4B). At one locality in the southeastern part of Berrheia, the biotitic metadike is undeformed and forms a planar body 1.5 to 2 m thick typical of dikes (trends N85°E, dips 35°S). At other localities, the metadikes are to varying degrees folded and even pinched out and broken. Moreover, metamorphic recrystallization has resulted in a biotite schistosity that is parallel or subparallel to the contacts of the metadikes. With few exceptions this schistosity has obliterated original igneous textures, although coarse grains in a few sections appear to be relict porphyritic plagioclase. Mafic minerals include hornblende, biotite, sphene, and in one section clinopyroxene. These characteristics of the younger dikes suggest that the surrounding gneiss as well as the dike rock were affected by amphibolite-facies metamorphism with deformation. Some of the younger metadikes are intruded by pink pegmatite. The younger biotitic metadike rocks appear to differ in petrographic character from the metadolerites in the western-central Sør Rondane Mountains (KOJIMA and SHIRAISHI, 1986; SHIRAISHI *et al.*, 1988).

3.11. Migmatite

Migmatites are widespread in Balchenfjella except the southern part. Agmatic, schollen, stromatic, folded, schlieren and nebulitic structures are characteristic (*e.g.* Plates

4C, 5A, B and C). Paleosomes of the migmatite consist mainly of the biotite-hornblende gneiss, amphibolite, and hornblende gneiss commonly with clinopyroxene; ultramafic and garnet-biotite gneiss paleosomes are rare. Neosomes of the migmatite range from leucocratic granite to granodiorite containing biotite, hornblende and locally clinopyroxene. These are commonly foliated due to parallel or subparallel orientation of the mafic minerals. The foliated neosomes cut the neighboring country gneisses in some places (Plate 5C).

4. Plutonic Rocks

4.1. Diorite

The diorite constitutes the easternmost nunatak of Firlingane, which appears black from a distance in contrast to nunataks composed of the metamorphic rocks (Plate 6A). The rock is dark-gray, medium- to coarse-grained and massive. The constituent minerals are, in decreasing abundance, plagioclase, biotite, hornblende, clinopyroxene and minor quartz, as well as accessory sphene, apatite, zircon, allanite and ore minerals. A trace amount of K-feldspar is locally present. Chlorite and epidote are common alteration products of biotite and plagioclase, respectively. Clinopyroxene is usually rimmed by green hornblende and paler green amphibole, possibly actinolite. Subophitic texture is observed in some samples.

The diorite contains xenoliths of quartzofeldspathic biotite-hornblende gneiss. Both rocks are cut by dikes of pink granite (Plate 6A).

4.2. Granite and pegmatite

Dikes and veins of granite and pegmatite are ubiquitous in the metamorphic rocks. These rocks are leucocratic, and usually massive but locally feebly gneissic. At least two stages of the granitic dikes and veins are recognizable: an earlier stage of white to light gray granite-pegmatite and a later stage of pink granite-pegmatite. The neosomes of the migmatite, together with the paleosomes, are cut by both stages of dikes and veins (Plate 6B).

5. Metamorphism

Mineral assemblages observed in the metamorphic rocks except the migmatite are listed in Table 1. This list is intended to serve as a summary of the mineralogy of the rocks examined in thin section. Minerals occurring together in a given section are included in the assemblage (obviously secondary or relict phases are distinguished), but in some cases, not all these minerals crystallized in equilibrium during a single metamorphic event (GREW *et al.*, 1989).

The orthopyroxene- and garnet-clinopyroxerne-bearing mineral assemblages (Plate 7A) are found over the area including Hesteskoen and Isrosene. The garnet-corundum (Plate 7B) and sillimanite-garnet-biotite-K-feldspar-plagioclase-quartz associations are characteristic of the area. Thus metamorphic grade attained the hornblende-granulite-facies of regional metamorphism. Kyanite and staurolite from Gropeheia are found as inclusions in garnet in the rocks of the assemblages C9 and C11, respectively (Plates 7C and 8A). The kyanite and staurolite are considered to be prograde relics in contrast to the retrograde kyanite reported by ASAMI and SHIRAISHI (1987) from the western Sør Rondane Mountains (GREW *et al.*, 1989; ASAMI *et al.*, 1990). In addition to these minerals, the estimated peak conditions of about 750°C and ≥7 kbar (GREW *et al.*, 1989; MAKIMOTO *et al.*, 1990) imply that the hornblende granulite-facies metamorphism in this area is probably of the medium pressure type as is the case in the western and central Sør Rondane Mountains (ASAMI and SHIRAISHI, 1987; OSANAI *et al.*, 1988; SHIRAISHI *et al.*, 1991).

Orthopyroxene and clinopyroxene in the metabasites and charnockitic gneiss are often partially replaced by cummingtonite and green hornblende or paler green amphibole (Plate 8B, C). Garnet is often embayed by biotite-plagioclase aggregates in the garnet-biotite gneiss and by hornblende-plagioclase aggregates in amphibolites and hornblende gneisses (Plate 8C). The replacement is more extensive in the more intensively migmatized areas, so that these primary minerals, particularly orthopyroxene, are rare in the migmatized area. Thus, the hornblende granulite-facies metamorphism is considered to have been followed by an amphibolite-facies metamorphism that is closely related with migmatization. Metamorphic temperatures around 600°C have been estimated for the later amphibolite-facies event (GREW *et al.*, 1989; ASAMI *et al.*, 1990; MAKIMOTO *et al.*, 1990).

Furthermore, high-temperature minerals, including amphiboles and biotite, listed in Table 1 are partially altered to low-temperature minerals such as calcite, chlorite, epidote, muscovite, and locally margarite and prehnite. These minerals suggest a late regressive stage in the greenschist facies.

6. Geological Structure

The metamorphic rocks of the Balchenfjella are highly deformed. On the outcrop scale, the most conspicuous structure is compositional layering. In rocks inferred to be of metasedimentary and metavolcanic origin, the layering is usually parallel to the boundaries between different rock types such as the pelitic gneiss and biotite-hornblende gneiss, so that the present layering is interpreted to reflect original layers in the sedimentary and volcanogenic precursors. Strikes and dips measured on the layering of the gneisses are shown by stereographic projections in Fig. 1, and representative structural data are plotted in the geological map.

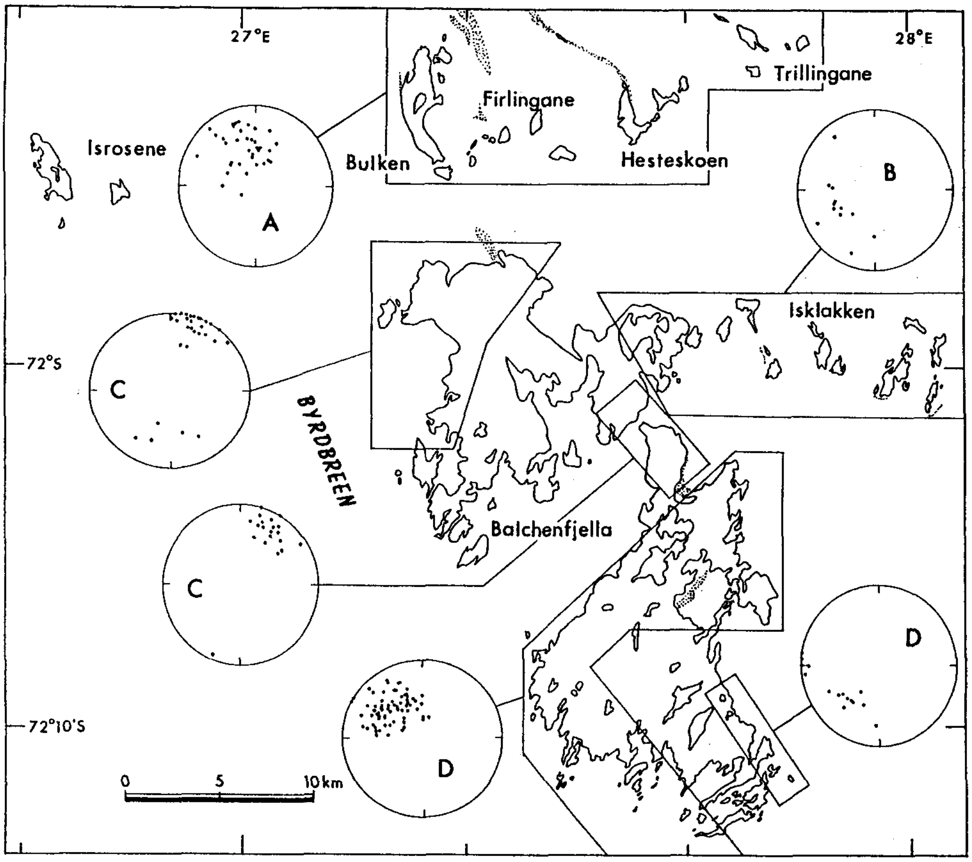

Fig. 1. Map showing stereographic plots of compositional layering in the metamorphic rocks. The letters A-D refer to four subareas each of which shows similar structural features.

Small scale folds are common in many outcrops. In many cases, these folds appear to be related to fault zones, which have displacements of several meters to 10 m, locally more (GREW *et al.*, 1988). On Balchenfjella, the metadikes and metagabbro, as well as the migmatites and gneisses, are deformed by these fault zones, in which the rocks are recrystallized as well as folded by dragging along the faults. These fault zones appear to be related to the later amphibolite-facies metamorphism and migmatization.

In order to better assess the distribution and extent of large scale (macroscopic) folds, we have divided the map area into four subareas that on the basis of the stereographic plots of the structural data have similar structural features (Fig. 1):

(A) Firlingane subarea
(B) Isklakken subarea
(C) Northern Balchenfjella subarea
(D) Southern Balchenfjella subarea

A macroscopic fold, an upright open antiform, is exposed at Gropeheia (Plate 6C). The fold axis lies within the migmatite belt and this fold deforms the foliation of the migmatite as shown in Plate 6C. Consequently, the subareas B and C are clearly correlated with each other. It is possible that subarea A is correlated with subarea B by a SE-trending synform presently covered by continental ice between Balchenfjella and Hesteskoen. The upright folds are inferred to be of a younger generation than recumbent folds found in nunataks, *e.g.* Vesthjelmen, northwest of this area (ASAMI *et al.*, 1989).

Subareas D are possibly parts of a unit distinct from the adjacent subarea C. Among the subareas D, the structures in the southeasternmost part, which is also a migmatite area, are somewhat different from the other part. This difference may be related to migmatization.

The timing suggests that the upright second generation folds and the fault zones could be related features, that is, deformation associated with the amphibolite-facies event and migmatization.

7. Metamorphic Evolution

On the basis of the results obtained from our geological and petrographic studies, we propose a tentative sequence of events.

(1) Deposition of sediments and volcanogenic rocks followed by emplacement of ultramafic rocks possibly as tectonically inserted mantle fragments.
(2) Magmatic activity, including emplacement of gabbroic and possibly pigeonite-bearing intrusions (Balchenfjella) and mafic (presently garnet-rich) dikes (Hesteskoen).
(3) Hornblende granulite-facies metamorphism.
(4) Magmatic activity, which involved emplacement of (presently biotitic) dikes of intermediate to basic composition.
(5) Amphibolite-facies metamorphism, migmatization, large scale open folding and extensive small scale deformation with development of fault zones.
(6) Plutonic activity, including diorite (Firlingane), and granitic dikes and veins.
(7) Greenschist-facies retrograde metamorphism, and formation of vein quartz with druses.

References

ANIYA, M. (1989): Landforms of the Balchenfjella area, the Sør Rondane, East Antarctica. Nankyoku Shiryô (Antarct. Rec.), **33**, 353-375.

ASAMI, M. and SHIRAISHI, K. (1987): Kyanite from the western part of the Sør Rondane Mountains, East Antarctica. Proc. NIPR Symp. Antarct. Geosci., **1**, 150-168.

ASAMI, M., MAKIMOTO, H., ANIYA, M., HAYASHI, M., IIMURA, Y., HAYASHI, T., NARAOKA, H., YONEZAWA, Y., FUJITA, S. and GREW, E.S. (1988): Sêru-Rondâne Sanchi chigaku chôsa hôkoku 1988 (JARE-29) (Report on the geological, geomorphological and geodetic field work and meteorite search in the Sør Rondane Mountains, 1988 (JARE-29)). Nankyoku Shiryô (Antarct. Rec.), **32**, 334-363.

ASAMI, M., MAKIMOTO, H. and GREW, E.S. (1989): Geology of the eastern Sør Rondane Mountains, East Antarctica. Proc. NIPR Symp. Antarct. Geosci., **3**, 81-99.

ASAMI, M., GREW, E.S. and MAKIMOTO, H. (1990): A staurolite-bearing corundum-garnet gneiss from the eastern Sør Rondane Mountains, Antarctica. Proc. NIPR Symp. Antarct. Geosci., **4**, 22-40.

GREW, E.S., ASAMI, M. and MAKIMOTO, H. (1988): Field studies in the eastern Sør Rondane Mountains, East Antarctica, with the 29th Japanese Antarctic Research Expedition (JARE). Antarct. J. U. S., **23**(5), 44-46.

GREW, E.S., ASAMI, M. and MAKIMOTO, H. (1989a): Preliminary petrological studies of the metamorphic rocks of the eastern Sør Rondane Mountains. Proc. NIPR Symp. Antarct. Geosci., **3**, 100-127.

GREW, E.S., ASAMI, M. and MAKIMOTO, H. (1989b): Aluminous and manganoan titanite from the Sør Rondane Mountains, East Antarctica. Antarct. J. U. S., **24**(5), 42-43.

HAYASHI, H. and MIURA, K. (1989): Glacial landforms and weathering processes in the Balchenfjella region, eastern part of the Sør Rondane Mountains, East Antarctica. Proc. NIPR Symp. Antarct. Geosci., **3**, 65-80.

ISHIZUKA, H. and KOJIMA, H. (1987): A preliminary report on the geology of the central part of the Sør Rondane Mountains, East Antarctica. Proc. NIPR Symp. Antarct. Geosci., **1**, 113-128.

KOJIMA, S. and SHIRAISHI, K. (1986): Note on the geology of the western part of the Sør Rondane Mountains, East Antarctica. Mem. Natl Inst. Polar Res., Spec. Issue, **43**, 116-131.

KRETZ, R. (1983): Symbols for rock-forming minerals. Am. Mineral., **68**, 277-279.

MAKIMOTO, H., ASAMI, M. and GREW, E.S. (1990): Metamorphic conditions of ultramafic lenses from the eastern Sør Rondane Mountains, East Antarctica. Proc. NIPR Symp. Antarct. Geosci., **4**, 9-21.

OSANAI, Y., TAKAHASHI, Y. and SAKIYAMA, T. (1988): High-grade metamorphic rocks from the central part of the Sør Rondane Mountains, East Antarctica (Abstract). Proc. NIPR Symp. Antarct. Geosci., **2**, 170.

OSANAI, Y., UENO, T., TSUCHIYA, N., TAKAHASHI, Y. and TAINOSHO, Y. (1990): Finding of vanadium-bearing garnet from the Sør Rondane Mountains, East Antarctica. Nankyoku Shiryô (Antarct. Rec.), **34**(3), 279-291.

PASTEELS, P. and MICHOT, J. (1970): Uranium-lead radioactive dating and lead isotope study on sphene and K-feldspar in the Sør Rondane Mountains, Dronning Maud Land, Antarctica. Eclogae Geol. Helv., **63**, 239-254.

PICCIOTTO, E., DEUTSCH, S. and PASTEELS, P. (1964): Isotopic ages from the Sør-Rondane Mountains, Dronning Maud Land. Antarctic Geology, ed by R.J. ADIE. Amsterdam, North-Holland, 570-578.

RAVICH, M.G. and KAMENEV, YE. N. (1972): Kristallicheskiy fundament Antarcticheskoy platformy (Crystalline Basement of the Antarctic Platform). Leningrad, Gidrometeoizdat, 658p.

SAKIYAMA, T., TAKAHASHI, Y. and OSANAI, Y. (1988): Geological and petrological characters of the plutonic rocks in the Lunckeryggen-Brattnipene region, Sør Rondane Mountains, East Antarctica. Proc. NIPR Symp. Antarct. Geosci., **2**, 80-95.

SHIRAISHI, K. and KOJIMA, S. (1987): Basic and intermediate gneisses from the western part of the Sør Rondane Mountains, East Antarctica. Proc. NIPR Symp. Antarct. Geosci., **1**, 129-149.

SHIRAISHI, K., KANISAWA, S. and ISHIKAWA, K. (1988): Geochemistry of post-orogenic mafic dike rocks from the eastern Queen Maud Land, East Antarctica. Proc. NIPR Symp. Antarct. Geosci., **2**, 117-132.

SHIRAISHI, K. and KAGAMI, H. (1989): Preliminary geochronological study of granulites from the Sør Rondane Mountains, East Antarctica - A comparison of Rb-Sr and Sm-Nd ages (Abstract). Proc. NIPR Symp. Antarct. Geosci., **3**, 152.

SHIRAISHI, K., ASAMI, M., ISHIZUKA, H., KOJIMA, H., KOJIMA, S., OSANAI, Y., SAKIYAMA, T., TAKAHASHI, Y., YAMAZAKI, M. and YOSHIKURA, S. (1991): Geology and metamorphism of the Sør Rondane Mountains, East Antarctica. Geological Evolution of Antarctica, ed. by M.R.A. THOMSON *et al.* Cambridge, Cambridge Univ. Press, 77-82.

TAKAHASHI, Y., ARAKAWA, Y., SAKIYAMA, T., OSANAI, Y. and MAKIMOTO, H. (1990): Rb-Sr and K-Ar whole rock ages of the plutonic bodies from the Sør Rondane Mountains, East Antarctica. Proc. NIPR Symp. Antarct. Geosci., **4**, 1-8.

TAKIGAMI, Y., KANEOKA, I. and FUNAKI, M. (1987): Age and paleomagnetic studies for intrusive and metamorphic rocks from the Sør Rondane Mountains, Antarctica. Proc. NIPR Symp. Antarct. Geosci., **1**, 169-177.

VAN AUTENBOER, T. (1969): Geology of the Sør-Rondane Mountains, Geologic Maps of Antarctica, ed. by C. CRADDOCK *et al.* New York, Am. Geogr. Soc., Pl. VIII (Antarct. Map Folio Ser., Folio 12, ed. by V.C. BUSHNELL).

VAN AUTENBOER, T., MICHOT, J. and PICCIOTTO, E. (1964): Outline of the geology and petrology of the Sør-Rondane Mountains, Dronning Maud Land. Antarctic Geology, ed. by R.J. ADIE. Amsterdam, North-Holland, 501-514.

VAN AUTENBOER, T. and LOY, W. (1972): Recent geological investigations in the Sør-Rondane Mountains, Belgicafjella and Sverdrupfjella, Dronning Maud Land. Antarctic Geology and Geophysics, ed. by R.J. ADIE. Oslo, Universitetsforlaget, 563-571.

A: Well-layered biotite-hornblende gneiss, northwest end of Gropeheia.

B: Hornblende gneiss (dark-colored) layers in biotite-hornblende gneiss, Firlingane.

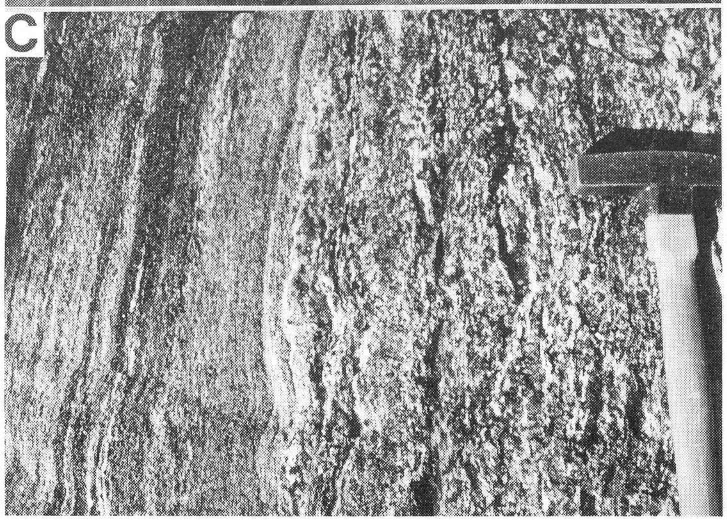

C: Garnet-biotite gneiss layer (right half) intercalated in biotite-hornblende gneiss, northeast end of Gropeheia.

Plate 2

A: Layered charnockitic gneiss, southeastern part of Berrheia.

B: Dolomitic marble layer with calc-silicate pods, north end of Berrheia.

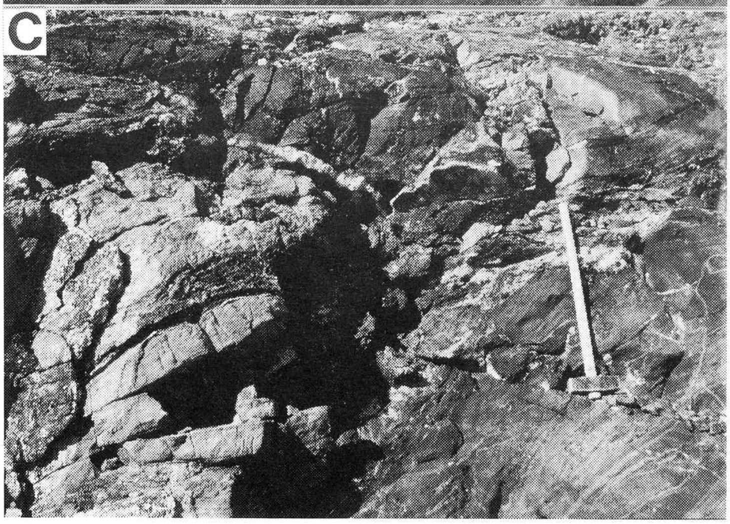

C: Ultramafic lens in biotite-hornblende gneiss, Gropeheia.

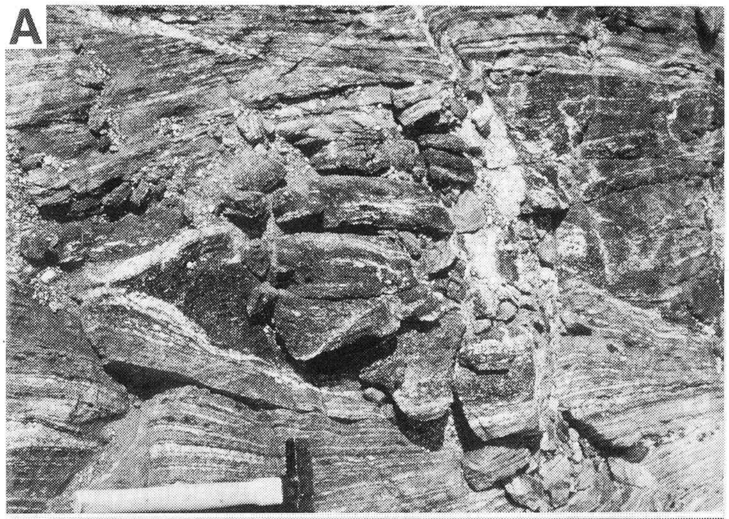

A: Amphibolite lens in biotite-hornblende gneiss, northwest end of Gropeheia.

B: Metagabbro lens (black knob) enclosed in a migmatite belt, north end of Berrheia. View from the north.

C: Metagabbro containing lath-shaped plagioclase crystals. The same locality as B.

Plate 4

A: Metadike of garnetiferous amphibolite broken into lenses, Hesteskoen. Layering of surrounding biotite-hornblende gneiss trends nearly parallel to the direction of the hammer handle.

B: Metadike of biotitic schist obliquely cutting biotite-hornblende gneiss, Firlingane.

C: Agmatic migmatite with biotite-hornblende gneiss paleosomes, western part of Gropeheia.

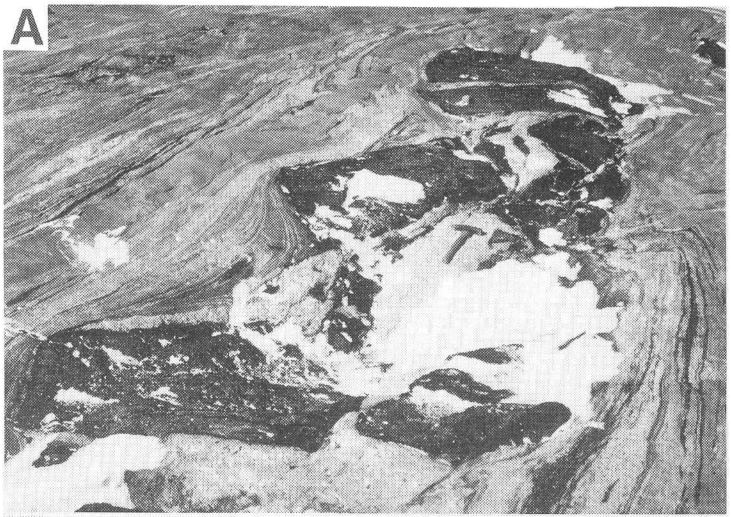

A: Stromatic migmatite with an ultramafic lens, southeastern part of Berrheia.

B: Migmatite with stromatic and folded structures, southeastern part of Gropeheia.

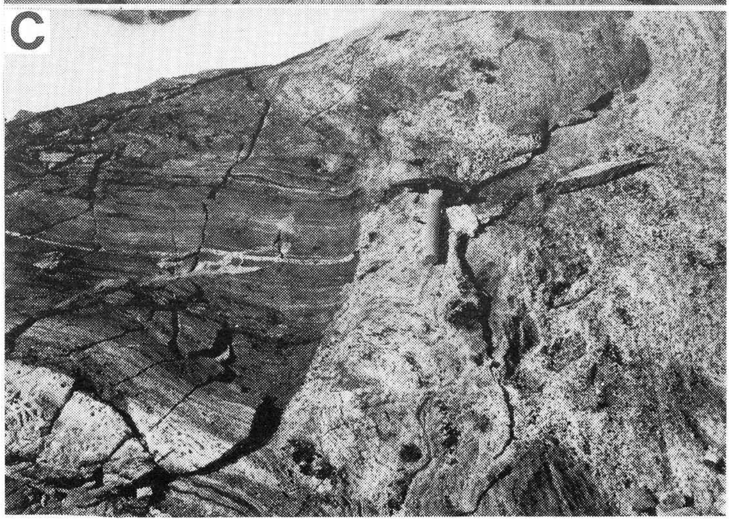

C: Discordant relation between nebulitic migmatite and adjacent gneisses, north end of Berrheia.

Plate 6

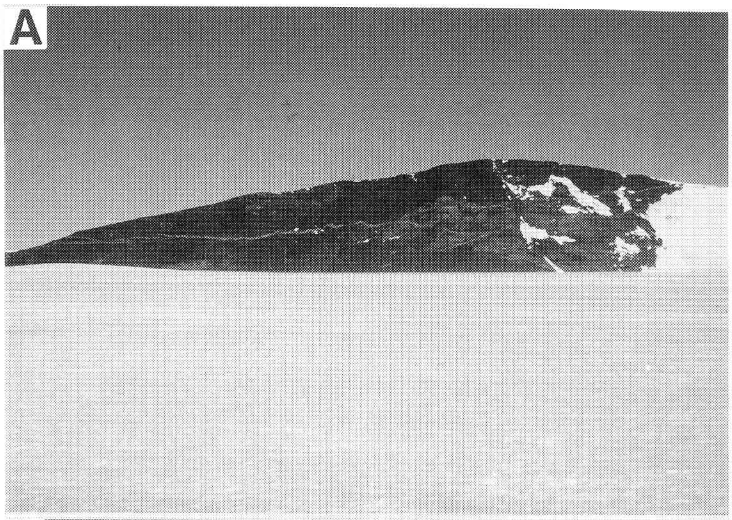

A: Diorite enclosing quartzofeldspathic biotite-hornblende gneiss, Firlingane, Both rocks are intruded by pink granite dikes.

B: Intrusive relation of an older, light gray granite dike and a younger, pink pegmatite dike in migmatite, southeastern part of Gropeheia.

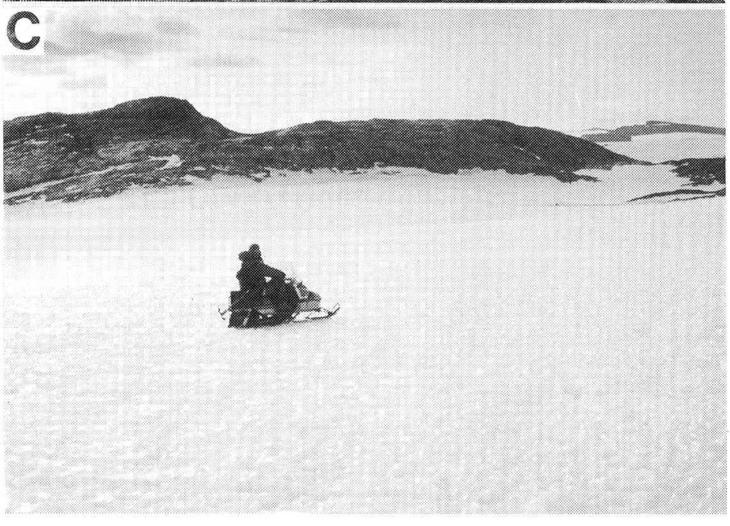

C: Open antiform in a migmatite belt, Gropeheia. View from the south. Width of the exposure is about 500 m.

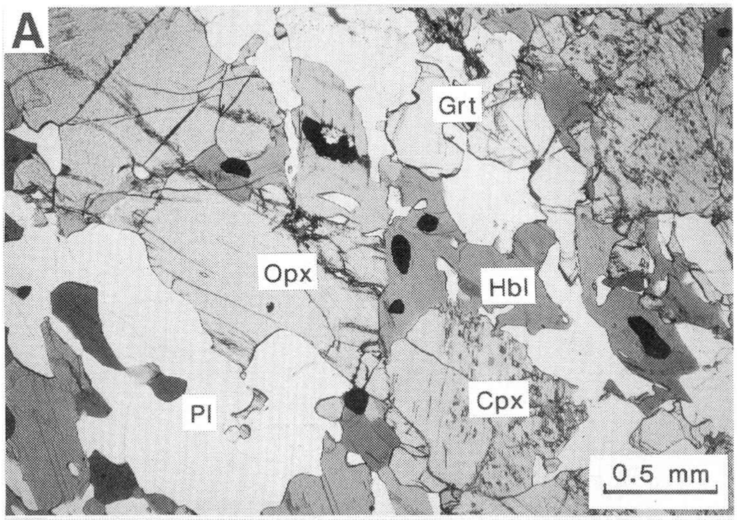

A: Photomicrograph of pyroxene granulite (MA88011826). Cpx: clinopyroxene, Grt: garnet, Hbl: hornblende, Opx: orthopyroxene, Pl: plagioclase. Mineral abbreviations are common in all photomicrographs. One nicol.

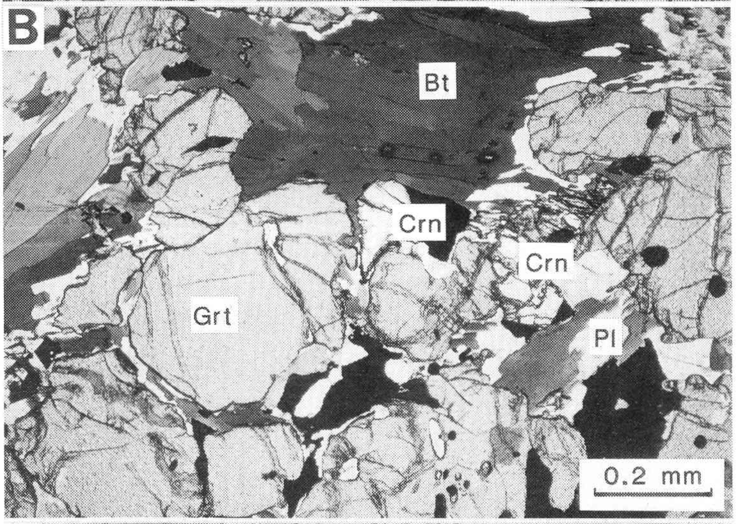

B: Photomicrograph of corundum-garnet gneiss (MA88011707). Bt: biotite, Crn: corundum. One nicol.

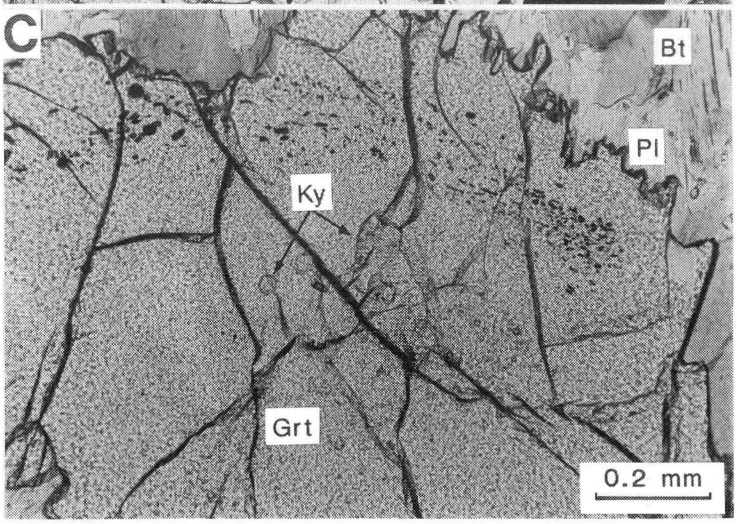

C: Photomicrograph of a garnet porphyroblast including kyanite (Ky) (plagioclase-garnet-biotite schist: HM88011803D). One nicol.

Plate 8

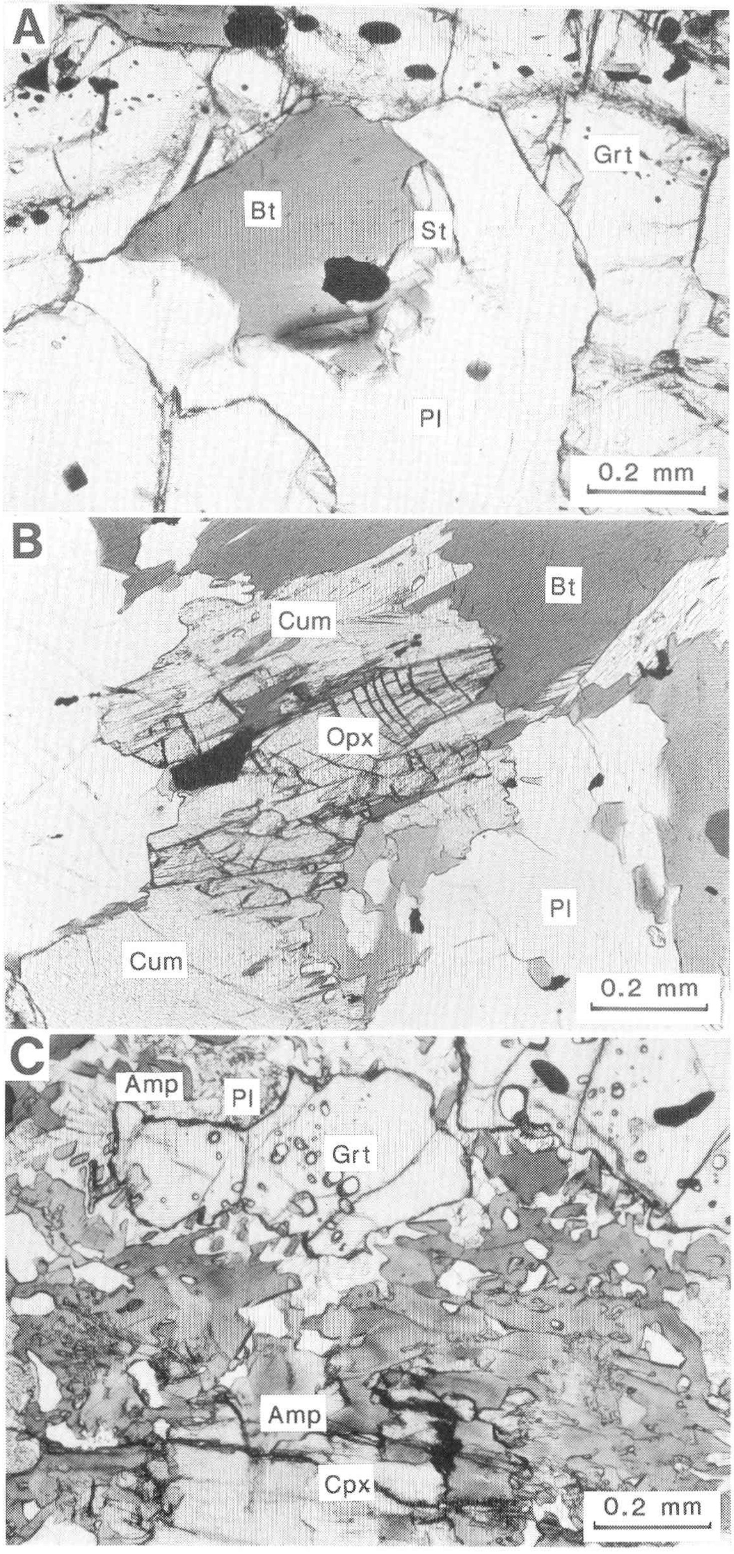

A: Photomicrograph of staurolite-bearing corundum-garnet gneiss (MA88011707-1). Staurolite grains (St) are associated with biotite and plagioclase which are included in a garnet porphyroblast. One nicol.

B: Photomicrograph of orthopyroxene-garnet-biotite gneiss (MA88012501). Orthopyroxene is rimmed by cummingtonite (Cum). One nicol.

C: Photomicrograph of garnet amphibolite (MA88011311). Garnet is embayed by pale green amphibole (Amp)-plagioclase aggregates and clinopyroxene is rimmed by pale green amphibole. One nicol.

Antarctic Geological Map Series

Sheet 1	East Ongul Island 1:5,000	March 1974
Sheet 2	West Ongul Island 1:5,000	March 1974
Sheet 3	Teöya 1:5,000	March 1975
Sheet 4	Ongulkalven Island 1:5,000	March 1975
Sheet 5	Langhovde 1:25,000	March 1976
Sheet 6 & 7	Skarvsnes 1:25,000	March 1977
Sheet 8	Kjuka and Telen 1:25,000	March 1979
Sheet 9	Skallen 1:25,000	March 1976
Sheet 10	Padda Island 1:25,000	March 1977
Sheet 11	Cape Hinode 1:25,000	March 1978
Sheet 12	Lützow-Holm Bay 1:250,000	March 1989
Sheet 13	Prince Olav Coast 1:250,000	March 1989
Sheet 14	Sinnan Rocks 1:25,000	March 1983
Sheet 15	Cape Ryûgû 1:25,000	March 1980
Sheet 16	Akebono Rock 1:25,000	March 1986
Sheet 17	Niban Rock 1:25,000	March 1983
Sheet 18	Kasumi Rock 1:25,000	March 1984
Sheet 19	Tenmondai Rock 1:25,000	March 1985
Sheet 20	Akarui Point and Naga-iwa Rock 1:25,000	March 1984
Sheet 21	Cape Omega 1:25,000	March 1979
Sheet 22	Oku-iwa Rock 1:25,000	March 1981
Sheet 23	Honnör Oku-iwa Rock 1:25,000	March 1987
Sheet 24	Rundvågskollane and Rundvågshetta 1:25,000	March 1986
Sheet 25	Botnneset 1:25,000	March 1987
Sheet 26	Strandnibba 1:25,000	March 1985
Sheet 27(1)	Mt. Fukushima, Northern Yamato Mountains 1:25,000	March 1978
Sheet 28	Central Yamato Mountains, Massif B and Massif C 1:25,000	March 1982
Sheet 29	Belgica Mountains 1:25,000	March 1981
Sheet 30	Southern Yamato Mountains (Massif A and JARE-IV Nunataks) 1:25,000	March 1988
Sheet 31	Balchenfjella 1:100,000	March 1991